



## Research article

# Synthesis, characterization, and cytotoxicity studies of nanocellulose extracted from okra (*Abelmoschus Esculentus*) fiber

Md. Tanvir Hossen<sup>a,\*\*</sup>, Chanchal Kumar Kundu<sup>a,\*</sup>, BM Riaz Rahman Pranto<sup>a</sup>,  
Md. Sifat Rahi<sup>b</sup>, Rajesh Chanda<sup>c</sup>, Swaraz Mollick<sup>a</sup>, Abu Bakr Siddique<sup>d</sup>,  
Hosne Ara Begum<sup>e</sup>

<sup>a</sup> Department of Textile Engineering, Jashore University of Science and Technology, Jashore, 7408, Bangladesh

<sup>b</sup> Department of Genetic Engineering and Biotechnology, Jashore University of Science and Technology, Jashore, 7408, Bangladesh

<sup>c</sup> Department of Chemical Engineering, Jashore University of Science and Technology, Jashore, 7408, Bangladesh

<sup>d</sup> Department of Textile Engineering, BGMEA University of Fashion & Technology, Dhaka, 1230, Bangladesh

<sup>e</sup> Department of Yarn Engineering, Bangladesh University of Textiles, Dhaka, 1208, Bangladesh

## ARTICLE INFO

## Keywords:

Okra fiber  
Nanocellulose  
Particle size  
Thermal properties  
Cytotoxicity

## ABSTRACT

Nanocellulose, especially originating from a natural source, has already shown immense potential to be considered in various fields, namely packaging, papermaking, composites, biomedical engineering, flame retardant, and thermal insulating materials, etc. due to its environmental friendliness and novel functionalities. Thus, a thorough characterization of nanocellulose is a hot research topic of research communities in a view to judge its suitability to be used in a specific area. In this work, a kind of green and environment-friendly nanocellulose was successfully prepared from okra fiber through a series of multi-step chemical treatments, specifically, scouring, alkali treatment, sodium chlorite bleaching, and sulfuric acid hydrolysis. Several characterization techniques were adopted to understand the morphology, structure, thermal behavior, crystallinity, and toxicological effects of prepared nanocellulose. Obtained data revealed the formation of rod-shaped nanocellulose and compared to raw okra fiber, their size distributions were significantly smaller. X-ray diffraction (XRD) patterns displayed that compared to the crystalline region, the amorphous region in raw fiber is notably larger, and in obtained nanocellulose, the crystallinity index increased significantly. Moreover, variations in the Fourier transform infrared spectroscopy (FTIR) peaks depicted the successful removal of amorphous regions, namely, lignin and hemicelluloses from the surface of fiber. Thermostability of synthesized nanocellulose was confirmed by both Differential Scanning Calorimetry (DSC) analysis, and thermogravimetric analysis (TGA). Cytotoxicity assessment showed that the okra fiber-derived nanocellulose exhibited lower to moderate cellular toxicity in a dose-dependent manner where the LD<sub>50</sub> value was 60.60 µg/ml.

\* Corresponding author.

\*\* Corresponding author.

E-mail addresses: [mth.te@just.edu.bd](mailto:mth.te@just.edu.bd) (Md.T. Hossen), [ck.kundu@just.edu.bd](mailto:ck.kundu@just.edu.bd) (C.K. Kundu).

<https://doi.org/10.1016/j.heliyon.2024.e25270>

Received 22 August 2023; Received in revised form 2 January 2024; Accepted 23 January 2024

2405-8440/© 2024 The Author(s). Published by Elsevier Ltd. This is an open access article under the CC BY-NC-ND license (<http://creativecommons.org/licenses/by-nc-nd/4.0/>).

## 1. Introduction

One of the most plentiful, biodegradable, and renewable natural biopolymers in the world is cellulose. Compared to single fibers, nano- and microscale fibrils produced from cellulosic fibers exhibit enhanced mechanical characteristics [1]. It is commonly known as nanowhiskers, nanocrystalline cellulose, or nanocrystals (CNC) and is derived from natural fibers or sea animals. In recent years, nano-cellulose obtained from various renewable sources has drawn more and more interest owing to its environmental benefits, low cost, better mechanical properties (high modulus and specific strength), greater specific surface area, and exceptional aspect ratio [2, 3]. Several researches have shown that nanocellulose can be used in composite material production, regenerative medicine, optics, and renewable energy storage devices [4,5].

Broadly, nanocellulose can be attained from different natural sources, such as wood [2], cotton [6], jute [7], ramie [8], sisal [9], okra [1], bacterial cellulose [10,11], wheat straw [12], bleached softwood pulps [13,14], coffee pulp [15], tunicate cellulose [16], and microcrystalline cellulose (MCC) [17]. However, among these resources jute, cotton, sisal, and ramie fibers possess great potential and demand as textile fibers. Moreover, over the last few decades these natural cellulose fibers have been the center of both commercial and research attention for their uses in the production of composite materials and day by day this demand is growing enormously [18]. Apart from them, Okra (*Abelmoschus Esculentus*) fiber, a lignocellulosic fiber, contains a large proportion of cellulose (nearly 55–70 %), hemicellulose (15–20 %), lignin (5–10 %), and pectin (3–5 %), along with certain water-soluble materials [19]. The applications of okra fibers in textile industries have a few downsides such as sensitivity to wear, poor fastness to rub as well as color, and a higher tendency to crease. Furthermore, previous studies demonstrated that common bleaching or alkalization chemical treatments failed to enhance the fiber's mechanical properties significantly for their probable use as fillers in composite materials [20–22]. This advocates that the usage of okra bast fibers as the raw material of nanocellulose can be a practical substitute for engaging them as technical fibers in textile products. The utilization of agro-waste for cellulose nanomaterials production along with textile fibers not only protects the ecology by employing biodegradable materials from renewable sources but also helps rustic societies to develop as farmers' crops get extra value, and this results in allotting more agricultural land for producing foods to feed our rising population as well [23].

In order to prepare nanocellulose including bacterial nanocellulose (BNC), cellulose nanocrystal (CNC), and cellulose nanofiber (CNF), different approaches are being followed by several researchers [24] such as the ionic liquid method [25], enzymatic method [26], TEMPO oxidative method [27], the mechanical method [28,29], combination method (mechanical with enzymatic hydrolysis or oxidation) [30,31], numerous acid hydrolysis such as formic [32], hydrochloric [33], phosphoric [34,35], sulfuric [36], mixed sulfuric acid/acetic acid [37], combined (sulfuric/oxalic acid) hydrolysis [38], and mixed chemical-ultrasonic treatments [39]. Cellulose nanomaterials can be made from each of these processes, based on the raw material's makeup and preparation, purification as well as disintegration process. Sulfuric acid hydrolysis is the most familiar approach for extracting nanocellulose.

The literature on the preparation of nano-cellulose from okra fibers is limited to a few studies. Usually, several chemical treatment processes, namely alkali treatment, double bleaching, and double sulfuric acid ( $H_2SO_4$ ) hydrolysis, are followed to extract nanocellulose from okra fiber [40]. Meanwhile, some common characterization techniques like Field-emission Scanning Electron Microscope (FESEM) and Infrared Spectroscopy (FT-IR) were adopted to confirm the formation of nanocellulose from okra fiber. However, it's some other important properties like size distribution and thermal behaviors were rarely studied. Even more, it is still not clear how the nanocellulose affects living beings, especially humans and animals including the environment [41]. So, it is necessary to measure the toxicological characteristics, including probable effects on people's health and safety [42,43]. Thus, all these above-mentioned characterizations are a time-demand task of the scientific community while considering their widespread usage in different wings of material and medical science industries.

Being inspired by the immense potential of nanocellulose to be considered in numerous applications of our daily necessities, we were motivated to develop nanocellulose from a naturally abundant okra plant with its detailed characterization. Here, in this study, nanocellulose is prepared from water-retted okra fibers by multistep chemical pretreatments supplemented by double sulfuric acid hydrolysis. The pretreatment processes were performed through scouring using soda and detergent, alkali treatment by sodium hydroxide, and double bleaching using sodium chlorite. Then the purified cellulose was hydrolyzed by means of sulfuric acid. The produced samples were characterized using TEM, DLS, XRD, FT-IR, TGA, DTG, and DSC techniques, and the synthesized nanocellulose samples' cytotoxicity assessment was carried out by a brine shrimp lethality test.

## 2. Experimental

### 2.1. Materials

The raw ingredient for the nanocellulose, okra bast fiber, was sourced from Jashore, Khulna region of Bangladesh. Detergent was sourced from the local market of Bangladesh and other necessary chemicals specifically sodium hydroxide (NaOH) (purity 99 %), sodium carbonate ( $Na_2CO_3$ ), sodium chlorite ( $NaClO_2$ ), glacial acetic acid ( $CH_3COOH$ ) (99.9 %) were bought from Merck, USA. Sulfuric acid ( $H_2SO_4$ ) with 98 % concentration, and dimethyl sulfoxide (DMSO) was obtained from Sigma-Aldrich, USA.

### 2.2. Nanocellulose preparation

The fiber was collected from mature okra plants of around 5 feet in height by retting in pond water for a period of 18–22 days [44]. A significant amount of green lignin part of the plant was separated by bacteria action, and okra fiber full of cellulose (almost 67 %) [45], became loosened. Then fiber was extracted manually, and the fiber was repeatedly cleaned in clean water and allowed to air dry

for roughly 48 h without exposure to sunlight. Around 28–30 cm of bottom fiber was discarded and the remaining fibers were sliced into three equal pieces (about 20 cm) namely top, middle, and bottom among which the middle portion was used for this experiment cutting the fibers as small as possible. Scouring of okra bast fiber was carried out in a solution containing surface-active agents such as 5 gm detergent and 5 mg  $\text{Na}_2\text{CO}_3$  for 1 L of water in a suitable beaker and it was a 1:50 ratio of fiber to solution [46]. For 30 min, the okra fiber solution was subjected to heating at 60 °C and then the fiber underwent multiple thorough washes in distilled water. After that, it is kept in a desiccator after being dried at 100–105 °C using an electrical oven. Synthesis of extracted cellulose fibers from okra was obtained via alkali treatment and bleaching which was done by dipping tiny fiber bundles in solutions containing 17.5 % concentrated NaOH at 40 °C for 120–130 min with constant shaking. Then, to get rid of extra NaOH, the fibers were passed through a filter cloth and cleaned with distilled water. For bleaching purposes, after being dried at 90 °C, the okra fiber underwent treatment with a 2 gm per liter (0.2 %) sodium chlorite ( $\text{NaClO}_2$ ) solution that was diluted in a known specified volume of water. The pH of the solution was 10.6, which was dropped to 4 by the use of acetic acid, and it took the digesting fiber over 2 h to complete the bleaching process. Finally, the fiber was stored in a desiccator after being cleaned with sufficient water and allowed to dry for approximately 4 h outside. Under identical circumstances, this procedure was performed once again. Hence, it is known as double bleaching. Following that, the extracted cellulose was filtered and repeatedly cleaned unless the samples' pH was neutral. After that, a freeze-dryer was utilized to carry out the drying process. For synthesizing nano-cellulose, the bleached cellulose was shortened to the smallest size feasible. In the end, okra cellulose underwent double-acid hydrolysis to produce nano-cellulose. The hydrolysis process was carried out at 400C using a 60 wt %  $\text{H}_2\text{SO}_4$  solution with constant stirring employing a magnetic stirrer on an electric hot plate, all while maintaining a 1:10 fiber-to-liquor ratio. After half an hour, 50 ml of ice-cold or distilled water was added to the mixture, which caused the hydrolysis to stop. Then, after 30 min of continuous stirring, the reaction mixture was allowed to cool to room temperature prior to centrifuging. Finally, the nanocellulose suspension was obtained by agitating the solid fraction while adding the necessary water. Absolute alcohol was used to keep the newly generated suspension in a clean safe glass vessel. All the above-mentioned processes (from the raw fiber collection to the preparation of nanocellulose fiber) are schematically presented in [Scheme S1](#) (see [APPENDIX A](#)).

### 2.3. Characterizations techniques

#### 2.3.1. Field- emission Scanning Electron Microscope (FESEM)

The morphological analysis of raw okra fiber and nano-cellulose was investigated using ZEISS Sigma 300 at a 5 kV accelerating voltage. Prior to analysis, a coating of gold was applied to the samples to avoid charging artefacts.

#### 2.3.2. Fourier transform infra-red spectroscopy analysis (FT-IR)

The FT-IR spectra were used to study the changes in chemical structures of the samples i.e. the chemical bonds present beforehand and following the hydrolysis processes of the samples. The FTIR spectra of raw okra fiber and nanocellulose were recorded on a Nicolet™ iSTM 10 FTIR spectrometer (Germany) at wavenumber within the range of 500–4000  $\text{cm}^{-1}$ .

#### 2.3.3. X-ray diffraction (XRD)

Utilizing Ni-filtered Cu  $K\alpha$  radiation operating at 40 kV and 30 mA, the diffraction patterns of raw okra fiber and nano-cellulose were examined in the range  $2\theta = 10\text{--}40^\circ$  using an Emperyan (Malvern PAN-alytical) x-ray diffractometer. The diffraction pattern was exploited to investigate the crystallinity index and equation (1) represents the calculation of the crystallinity index using the Segal empirical approach [47]:

$$\text{CrI} = \frac{I_{200} - I_{\text{am}}}{I_{200}} \times 100\% \quad (1)$$

where  $I_{\text{am}}$  represents the amorphous cellulose's intensity at about  $2\theta = 18\text{--}19^\circ$  and  $I_{200}$  denotes the crystallites peak's intensity at approximately  $2\theta = 22.5^\circ$

#### 2.3.4. Transmission electron microscopy (TEM)

The Talos™ F200X G2 TEM, operating between 120 and 200 kV, was used to analyze the size dimensions and structure of nano-celluloses. For analysis, a droplet of 10  $\mu\text{L}$  of nano-cellulose suspension was taken on copper grids that had a film of carbon covering them. Using the TEM images, the diameter of the particles was calculated using an effective software named ImageJ.

#### 2.3.5. Thermogravimetric analysis (TGA)

Thermogravimetric measurements were performed by using a STA 449 F1 Jupiter® tool. Dynamic test temperature programs were executed at a heating rate of 10 °C/min from 25 °C to 700 °C. A nitrogen atmosphere (20 ml/min) was used during these tests to avoid thermo-oxidative deterioration.

#### 2.3.6. Dynamic light scattering (DLS)

The dimensions of nano-cellulose obtained from okra fiber were assessed by using a Zetasizer Advance Range instrument. An UltraTurrax device (Germany) was used for the dilution and dispersion of nanocellulose samples before DLS measurements and suspended bubbles were removed by means of ultrasonication. A critical approach was displayed during the whole process of measuring nano-cellulose dimensions by DLS.

### 2.3.7. Differential scanning calorimetry (DSC)

DSC runs were performed in an STA 449 F1 Jupiter® with a nitrogen environment, starting from room temperature and increasing up to 400 °C at a rate of 2 °C/min heating.

### 2.3.8. Cytotoxicity study

Brine Shrimp Lethality Test was carried out for the cytotoxicity assessment of the nanocellulose samples in a dose-dependent manner and the LD<sub>50</sub> value was calculated from a graph, the regression line was generated with an equation. Here, a brine shrimp nauplii lethality test was performed to determine the cytotoxic effect of the nanocellulose extracted from okra fiber, according to the standard procedure with a slight modification [48]. The test organism was brine shrimp eggs obtained from the local market. The beaker was filled with artificial saltwater, and 0.50 g of shrimp eggs were placed to one side before it was covered. The shrimp were given 48 h to develop into larvae (nauplii), and an oxygen supplier ensured a steady supply of oxygen during this hatching stage. These nauplii were taken for the cytotoxicity assay. A lamp was fixed just above the beaker for shrimp attraction so that nauplii broke the eggshell and got free. The nauplii were taken from the beaker by a dropper and 10 nauplii were taken carefully by micropipette. 1 mg/ml Stock solution of nanocellulose was prepared by adding 0.01 % DMSO with saline water. Then clean test tubes were taken for different concentrations for the test samples. The aliquots of 5 concentrations (5, 10, 25, 50, 100 µg/ml) were made by serial dilution technique for nanocellulose solutions. The final volume of the solution in each test tube was 10 ml using saline water. Then the test tubes were incubated for 24 h in an ambient condition. After 24 h of incubation, the surviving nauplii were counted by observing through a magnifying glass against a white background. The concentration of the sample needed to eliminate 50 % of the brine shrimp population is known as the LD<sub>50</sub> (50 % lethal dosage) value, which was determined by plotting the concentration of okra nano-cellulose against the plot of inhibition. For every concentration and control, the percentage of nauplii lethality was computed, and the percentage of death was determined by counting the number of dead and live nauplii in each tube.

$$\text{Percentage of Death} = \left[ \frac{\text{Quantity of dead nauplii}}{\text{Quantity of dead nauplii} + \text{Quantity of living nauplii}} \right] \times 100$$

Finally, the LD<sub>50</sub> value is calculated through the regression line of the graph with a plot of mortality % against different concentrations.

## 3. Results and discussion

### 3.1. X-ray diffraction (XRD) analysis

In Fig. 1, the XRD patterns of raw okra fiber and nano-cellulose are demonstrated. In the case of raw fiber, several diffraction peaks at around  $2\theta \approx 12^\circ$ ,  $20^\circ$  and  $22^\circ$  are present. Meanwhile, for the nano-cellulose, a sharp peak at about  $2\theta \approx 23^\circ$  is detected apart from a minor peak at around  $17^\circ$ . Here, the peak present in a range from  $17^\circ$  to  $23^\circ$  represents the existence of typical cellulose I. Meanwhile, the corresponding crystallinity index (CI) is calculated from these XRD peaks where the raw okra fiber exhibits its crystalline nature in a very small margin likely ca. 5.5 % (see Table 1). Alternatively, the as prepared nano-cellulose has a bit higher crystallinity %, which is around 29 % (see Table 1). Such an increase in crystallinity index % for the okra nano-cellulose fiber compared to its pristine form indicates the elimination of amorphous moieties from the raw fiber throughout the acid hydrolysis process [49]. Thus, the XRD patterns indicate that this hydrolysis process keeps the crystalline cellulose intact while destroying the amorphous cellulose compounds, which is reasonably desirable in this work.

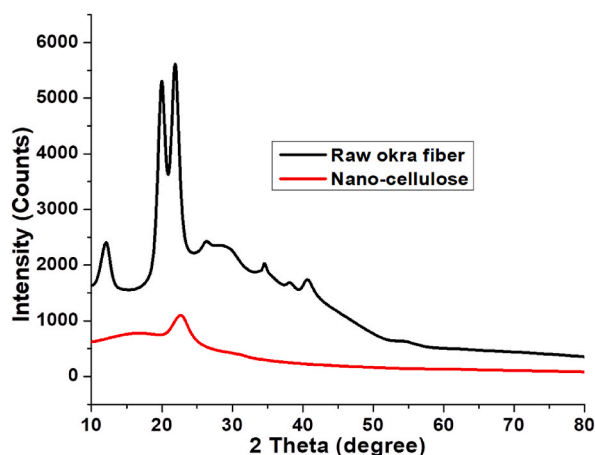


Fig. 1. XRD patterns of both raw okra fiber and nano-cellulose extracted from okra.

**Table 1**  
Crystallinity Index (%) of raw okra fiber and extracted nanocellulose.

Sample	Crystallinity Index (CrI) (%)
Raw okra fiber	5.52 %
Okra Nano-cellulose	29.21 %

### 3.2. Fourier transform-infrared (FT-IR) spectroscopy analysis

In Fig. 2, FT-IR spectra of raw okra fiber, and nano-cellulose are shown. Both spectra have peaks at around  $3400\text{ cm}^{-1}$  representing  $\text{-OH}$  stretching, at about  $2890\text{ cm}^{-1}$  representing  $\text{C-H}$  stretching, and at nearly  $1730\text{ cm}^{-1}$ , which may be due to the  $\text{C=O}$  stretching resulting from lignin and hemicellulose fragment, and at around  $1000\text{-}1100\text{ cm}^{-1}$  representing  $\beta\text{-glycoside}$ . However, the absence of peaks at  $1240\text{ cm}^{-1}$ ,  $1456\text{ cm}^{-1}$ , and  $1735\text{ cm}^{-1}$  is missing from nano-cellulose spectra suggesting the exclusion of hemicellulose and lignin (see Table 2), which also indicates the successful formation of nano-cellulose [50–52].

### 3.3. Field emission scanning electron microscopy (FESEM) and transmission electron microscopy (TEM) analysis

Fig. 3 shows the presence of lengthwise aligned unit cells with orientations that are substantially parallel in raw okra fiber. Surface roughness is the result of the cemented material, lignin and fatty compounds, filling the intercellular space ununiformly and holding the unit cells tightly in a fiber [40,44]. Moreover, the existence of porosity on the surface of fiber was found and it is visible that raw okra fiber has a diameter of around  $150\text{--}300\text{ }\mu\text{m}$  (see Fig. 3a) and as-prepared nano-cellulose diameter is between a range of about  $40\text{--}80\text{ nm}$  with some micro-cellulose (see Fig. 3b). As a consequence of the exclusion of lignin, surface impurities, and hemicellulose, images of nano-cellulose appear to be smoother and free from surface roughness. In addition, the TEM image of nano-cellulose [see Fig. 3 (c-e)] further confirms the shape of around  $29\text{--}33\text{ nm}$  diameter-sized nanocellulose fiber, and these diameters were analyzed by ImageJ software. Some parts of the crystalline areas and amorphous domains of cellulose were eradicated by the hydrolysis process and it led to the creation of rod-shaped nano-scaled cellulose fibers [46,53].

### 3.4. Thermogravimetric analysis (TGA)

Obtained okra nano-cellulose's thermal behaviors are investigated through TGA and derivative thermogravimetric (DTG) analysis. The relevant curves of TGA and DTG are depicted in Fig. 4. From Fig. 4, it is revealed that the raw okra fiber starts to decompose at around  $25\text{ }^\circ\text{C}$  and its initial weight loss remains last up to  $120\text{ }^\circ\text{C}$ , corresponding to the release of moisture and adsorbed water by the fiber itself [54,55]. However, for the okra nano-cellulose, this breakdown happens in a bit different way where the initial decomposition continues in a longer temperature spectrum starting from  $50\text{ }^\circ\text{C}$  up to  $250\text{ }^\circ\text{C}$ , which is possibly due to the presence of a big amount of crystalline content in the prepared nano-cellulose [56].

Such phenomena logically support the XRD test data as mentioned earlier. Moreover, the major weight loss generates around  $130\text{ }^\circ\text{C}\text{--}370\text{ }^\circ\text{C}$  and  $260\text{--}370\text{ }^\circ\text{C}$  for the raw fiber and nano-cellulose, correspondingly, which is owing to the degradation of hemicellulose, lignin, and cellulose content [57]. In addition, about the residue %, it is seen that the okra nano-cellulose leaves a higher char residue % compared to the virgin okra fiber, which is nearly  $11\%$  and  $27\%$  for the raw fiber and the nano-cellulose, respectively,

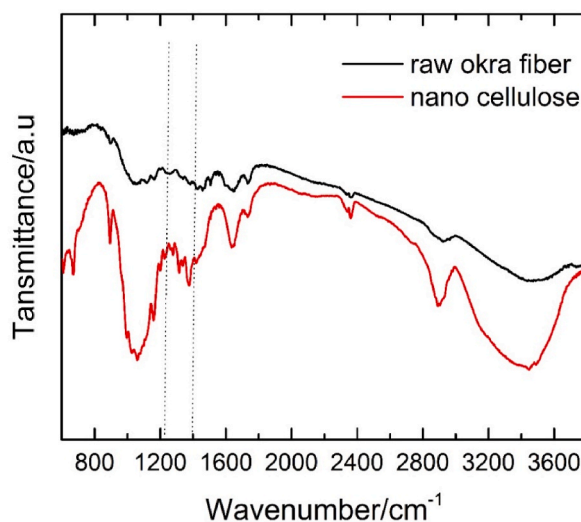
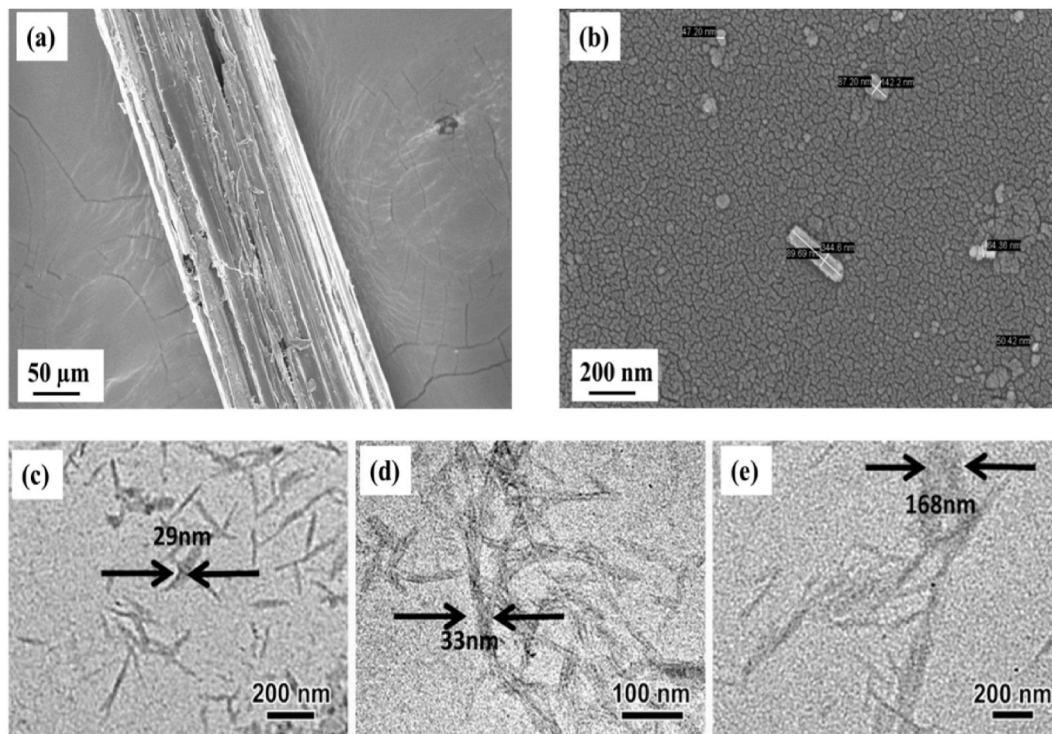


Fig. 2. FT-IR spectra of nano-cellulose along with raw okra fiber.

**Table 2**  
Absorption bands of cellulose, hemicellulose, and lignin's functional groups [50].

Component	Wave number (cm <sup>-1</sup> )	Functional group	Compounds
Cellulose, Hemicellulose, Lignin	4000–2995	OH	Acid, methanol
	2890	C–H	Alkyl, aliphatic
Hemicellulose, Lignin	1765–1730	C=O	Ketone and carbonyl, Aromatic
Cellulose,	1640	Fiber–OH	Adsorbed water
Lignin	1632	C=C	Benzene stretching ring
	1,613, 1450	C=C	Aromatic skeletal mode
	1430	O–CH <sub>3</sub>	Methoxyl– O–CH <sub>3</sub>
Cellulose, Lignin	1270–1215	C–O–C	Aryl-alkyl ether
Cellulose, Hemicellulose, Lignin	1108–1000	OH	C–OH



**Fig. 3.** FESEM images of (a) raw okra fiber and (b) nano-cellulose; TEM images of nanocellulose (c–e).

indicating better thermal stability of as obtained nano-cellulose. This is because of the presence of sulphate group in okra nano-cellulose fibers, which in turn exhibits its flame inhibition efficacy via producing char residues during the decomposition process in a higher temperature range [58]. Meanwhile, maximum value of degradation temperatures expressed as  $T^{\max}$  of raw fiber and its nano-cellulose are 330 and 350 °C as observed from DTG curves [see Fig. 4b]. These findings support the notion that nano-cellulose has greater heat stability than raw fiber.

### 3.5. Differential scanning calorimetry analysis (DSC)

The differential scanning calorimetry (DSC) test is carried out to study the changes of physical properties as well as the nature of the decomposition of fiber materials along with temperature against time and the obtained curves are depicted in Fig. 5.

From Fig. 5, it is seen that the raw okra fiber exhibits a broad exothermic peak located at around 25 °C–140 °C for raw okra fiber indicating the fact the phenomenon of heat release during the water evaporation process [59]. Meanwhile, for the nano-cellulose fiber, a smaller exothermic peak is observed at two different temperatures, namely at 50 °C and 350 °C and all these data closely match with the data obtained from the TGA analysis. In the later stage, say after 140 °C and 350 °C (in the case of raw fiber and nano-cellulose, respectively), a significant change in physical properties likely depolymerization of tested materials happens [60]. Since it is believed that the thermal decomposition process of cellulosic materials usually initiates in amorphous regions and gradually progresses to the crystalline regions, so, the raw fiber starts to decompose at a lower temperature range due to its higher amorphous contents than the

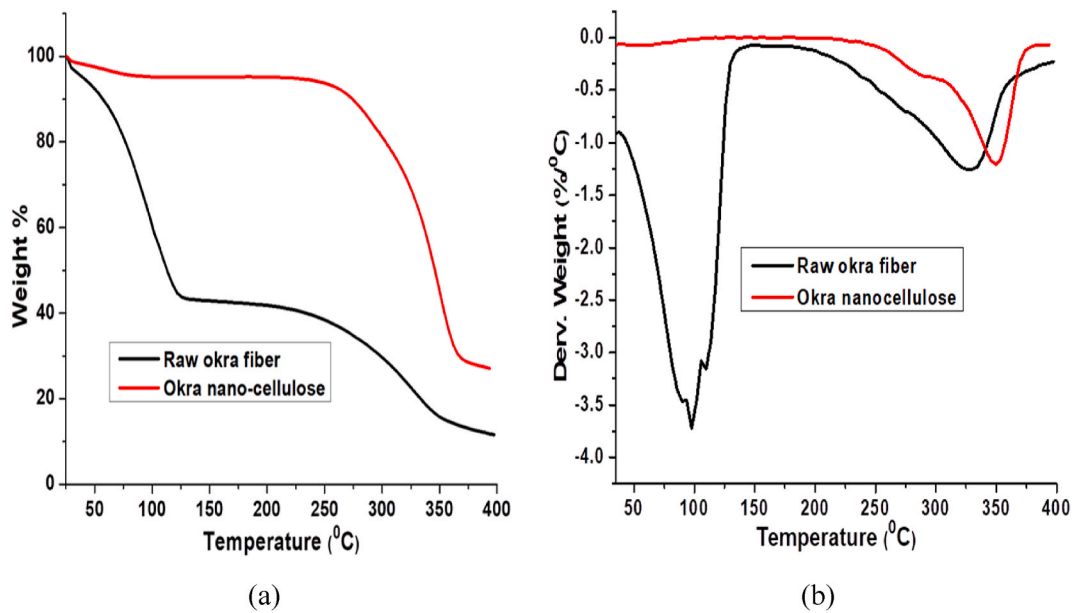


Fig. 4. Thermogravimetric Analysis (TGA) curves included the thermogravimetric (TG) (a) and derivative thermogravimetric (DTG) (b) curves of both raw okra fiber and okra nano-cellulose.

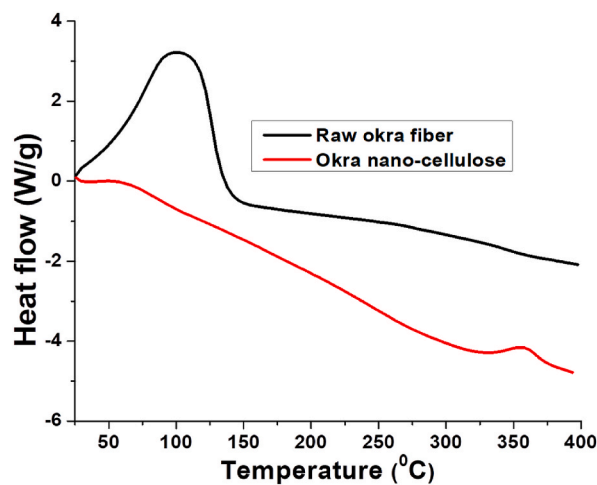


Fig. 5. DSC curves of both raw okra fiber and okra nano-cellulose.

nano-crystalline cellulose.

### 3.6. Dynamic light scattering analysis (DLS)

A really common, highly effective, and non-destructive method is DLS to address particle size [61]. Fig. 6 demonstrates the intensity-weighted size distribution of particles available from the solution of okra raw fiber and okra nano-cellulose.

Here, the okra nano-cellulose fibers exhibit a major and a smaller peak, where the major one with an average of 190 nm with an intensity of ca. 25 % and the smaller one with a mean value of 28.2 nm with an intensity of ca. 2 %. This result also validates the successful production of nano-sized fibers. In addition, the smaller range and narrower distribution of okra nano-cellulose fibers indicate that the as-developed nano-cellulose particles are uniform in size and well-dispersed in solution.

### 3.7. Cytotoxicity testing activity

In the brine shrimp lethality assay, the experimental sample of nanocellulose exhibited moderate cytotoxicity (see Fig. 7). From

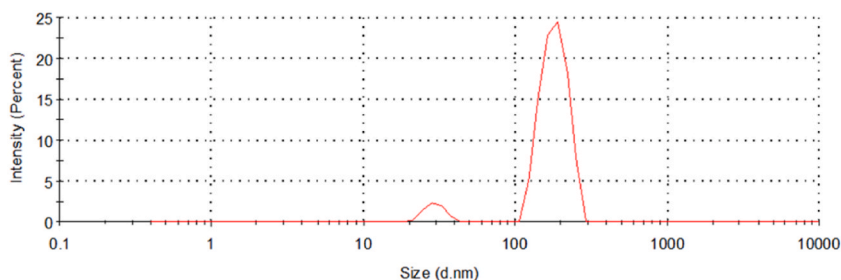


Fig. 6. DLS of nano-cellulose extracted from okra.

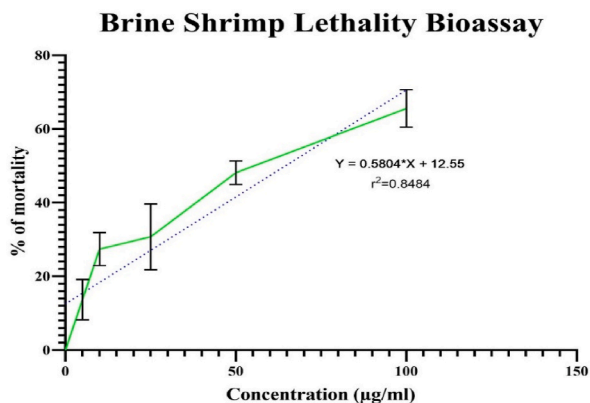


Fig. 7. Cytotoxic activity of nanocellulose.

Fig. 7, it is shown that the shrimp mortality is gradually elevated in a dose-dependent manner. The mortality is below 30 % up to the concentration of 25 µg/ml, whereas around 50 % of shrimp were alive at 50 µg/ml concentration. The mortality increased to above 60 % when 100 µg/ml nanocellulose was applied. From the graph, the regression line is generated with an equation which is followed by used to determine the LD<sub>50</sub> value. The LD<sub>50</sub> value is 60.60 µg/ml. The result manifested that the experimental sample would be toxic in high concentrations whereas the lower concentration could be nontoxic or minutely toxic to biological samples.

Here, the mortality percentage of nanocellulose was taken at different concentrations. The LD<sub>50</sub> values were calculated from the regression equation. For each tested dosage, the data are shown as mean ± SD (n = 3).

#### 4. Conclusions

Nano-cellulose was synthesized from agricultural waste okra fiber through a series of chemical pretreatments and double sulfuric acid hydrolysis. The successful creation of nano-cellulose was established via FESEM and TEM images accompanied by the DLS technique. The effective elimination of most hemicellulose and lignin was established by the FTIR spectra and The XRD patterns depicted the higher crystallinity of nano-cellulose than raw okra fibers. Moreover, TGA and DSC data analyzed the thermostability of the obtained nanoparticles sample. The brine shrimp lethality test showed lower to moderate cytotoxicity at a concentration of around 60.60 µg/ml (LD<sub>50</sub> value) below which the extracted nano-cellulose exhibited non-toxicity. The limitations of this study are the inability to perform an AFM analysis of prepared nanocellulose from water-retted okra bast fibers and not using any vivo, animal system, such as human cell line controlling different conditions for assessing toxicity to apply them in biomedical and functional textiles [62]. The AFM test, which could lead to the unraveling of the 3D structure of extracted nanocellulose, and testing toxicity in vivo, especially in human cell lines, are worthy of future research to study the potential carcinogenic effect, which must consider the mechanism of exposure, dose, and response, different periods of exposure, and severity of effects.

#### Notes

The authors announce no financial conflicts of interest.

#### Funding statement

This study was supported by Jashore University of Science and Technology.

## Data availability statement

Data included in article/supplementary material/referenced in article.

## CRediT authorship contribution statement

**Md. Tanvir Hossen:** Writing – original draft, Methodology, Formal analysis, Data curation, Conceptualization. **Chanchal Kumar Kundu:** Writing – review & editing, Writing – original draft, Supervision, Conceptualization. **BM Riaz Rahman Pranto:** Writing – original draft, Resources, Data curation. **Md. Sifat Rahi:** Writing – original draft, Methodology, Formal analysis. **Rajesh Chanda:** Writing – original draft, Methodology, Formal analysis. **Swaraz Mollick:** Writing – review & editing, Formal analysis. **Abu Bakr Siddique:** Writing – review & editing. **Hosne Ara Begum:** Supervision, Project administration, Conceptualization.

## Declaration of competing interest

The authors declare that they have no known competing financial interests or personal relationships that could have appeared to influence the work reported in this paper.

## Appendix A. Supplementary data

Supplementary data to this article can be found online at <https://doi.org/10.1016/j.heliyon.2024.e25270>.

## References

- [1] E. Fortunati, D. Puglia, M. Monti, C. Santulli, M. Maniruzzaman, J.M. Kenny, Cellulose nanocrystals extracted from okra fibers in PVA nanocomposites, *J. Appl. Polym. Sci.* 128 (2013) 3220–3230, <https://doi.org/10.1002/app.38524>.
- [2] Y. Habibi, L.A. Lucia, Rojas, Cellulose nanocrystals: chemistry, self-assembly, and applications, *Chem. Rev.* 110 (2010) 3479, <https://doi.org/10.1021/cr900339w>.
- [3] M.M. de Souza Lima, R. Borsali, Rodlike, Cellulose microcrystals: structure, properties, and applications, *Macromol. Rapid Commun.* 25 (2004) 771–787, <https://doi.org/10.1002/marc.200300268>.
- [4] K. Fleming, D.G. Gray, S. Matthews, Cellulose Crystallites. *Chem. Eur. J.* 7 (2001) 1831–1836, [10.1002/1521-3765\(20010504\)7:9<1831::AID-CHEM1831>3.0.CO;2-S](https://doi.org/10.1002/1521-3765(20010504)7:9<1831::AID-CHEM1831>3.0.CO;2-S).
- [5] C.K. Maity, S. De, K. Verma, M. Moniruzzaman, S. Sahoo, Nanocellulose: a versatile nanostructure for energy storage applications, *Ind. Crops Prod.* 204 (2023) 117218, <https://doi.org/10.1016/j.indcrop.2023.117218>.
- [6] X.M. Dong, J.F. Revol, D.G. Gray, Effect of microcrystallite preparation conditions on the formation of colloid crystals of cellulose, *Cellulose* 5 (1998) 19–32, <https://doi.org/10.1023/A:1009260511939>.
- [7] Saeed M. Jahan, H. Abrar, N. Zhibin, Yonghao, Jute as raw material for the preparation of microcrystalline cellulose, *Cellulose* 18 (2011) 451–459, <https://doi.org/10.1007/s10570-010-9481-z>.
- [8] Antonio Curvelo, de Menezes, Aparecido & Dufresne, Alain & Siqueira, Gilberto. Extrusion and characterization of functionalized cellulose whisker reinforced polyethylene nanocomposites, *Polymer* 50 (2009), <https://doi.org/10.1016/j.polymer.2009.07.038>.
- [9] J.I. Morán, V.A. Alvarez, V.P. Cyras, et al., Extraction of cellulose and preparation of nanocellulose from sisal fibers, *Cellulose* 15 (2008) 149–159, <https://doi.org/10.1007/s10570-007-9145-9>.
- [10] Jun Araki, Shigenori Kuga, Effect of trace electrolyte on liquid crystal type of cellulose microcrystals, *Langmuir* 17 (15) (2001) 4493–4496, <https://doi.org/10.1021/la0102455>.
- [11] M. Roman, W.T. Winter, Effect of sulfate groups from sulfuric acid hydrolysis on the thermal degradation behavior of bacterial cellulose, *Biomacromolecules* 5 (5) (2004) 1671–1677, <https://doi.org/10.1021/bm034519+>.
- [12] W. Helbert, C.Y. Cavallé, A. Dufresne, Thermoplastic nanocomposites filled with wheat straw cellulose whiskers. Part I: processing and mechanical behavior, *Polym. Compos.* 17 (1996) 604, <https://doi.org/10.1002/pc.10650>.
- [13] J. Araki, M. Wada, S. Kuga, et al., Influence of surface charge on viscosity behavior of cellulose microcrystal suspension, *J. Wood Sci.* 45 (1999) 258–261, <https://doi.org/10.1007/BF01177736>.
- [14] S. Beck-Candanedo, M. Roman, D.G. Gray, Effect of reaction conditions on the properties and behavior of wood cellulose nanocrystal suspensions, *Biomacromolecules* 6 (2) (2005) 1048–1054, <https://doi.org/10.1021/bm049300p>.
- [15] S. Malarat, D. Khongpun, K. Limtong, N. Sinthuwong, P. Soontornapaluk, C. Sakdaronnarong, P. Posoknistakul, Preparation of nanocellulose from coffee pulp and its potential as a polymer reinforcement, *ACS Omega* 8 (28) (2023) 25122–25133, <https://doi.org/10.1021/acsomega.3c02016>.
- [16] V. Favier, H. Chanzy, J.Y. Cavaille, Polymer nanocomposites reinforced by cellulose whiskers, *Macromolecules* 28 (1995) 6365–6367, <https://doi.org/10.1021/ma00122a053>.
- [17] D. Bondeson, A. Mathew, K. Oksman, Optimization of the isolation of nanocrystals from microcrystalline cellulose by acid hydrolysis, *Cellulose* 13 (2006) 171, <https://doi.org/10.1007/s10570-006-9061-4>.
- [18] D. Stawski, E. Çalişkan, N.D. Yilmaz, I. Krucińska, Thermal and mechanical characteristics of okra (*Abelmoschus esculentus*) fibers obtained via water- and dew-retting, *Appl. Sci.* 10 (2020) 5113, <https://doi.org/10.3390/app10155113>.
- [19] I.M. De Rosa, J.M. Kenny, D. Puglia, C. Santulli, F. Sarasini, Morphological, thermal and mechanical characterization of okra (*Abelmoschus esculentus*) fibres as potential reinforcement in polymer composites, *Compos. Sci. Technol.* 70 (2010) 116–122, <https://doi.org/10.1016/j.compscitech.2009.09.013>.
- [20] I.M. De Rosa, J.M. Kenny, M. Maniruzzaman, M. Moniruzzaman, M. Monti, D. Puglia, C. Santulli, F. Sarasini, Effect of chemical treatments on the mechanical and thermal behaviour of okra (*Abelmoschus esculentus*) fibres, *Compos. Sci. Technol.* 71 (2011) 246–254, <https://doi.org/10.1016/j.compscitech.2010.11.023>.
- [21] G.M. Arifuzzaman Khan, N.D. Yilmaz, K. Yilmaz, Okra bast fiber as potential reinforcement element of biocomposites: can it be the flax of the future, in: *Handbook of Composites from Renewable Materials*, Wiley Scrivener, Hoboken, MA, USA, 2017, pp. 379–405, <https://doi.org/10.1002/9781119441632.ch77>.
- [22] A.A. Mohana, M.A. Rahman, M.H. Rahaman, M. Maniruzzaman, S.M. Farhad, M.M. Islam, M.S.I. Khan, M.Z. Parvez, Okra micro-cellulose crystal (MCC) and micro-clay composites for the remediation of copper, nickel, and dye (basic yellow II) from wastewater, *Reactions* 4 (3) (2023) 342–358, <https://doi.org/10.3390/reactions4030021>.

- [23] G.M.A. Khan, N.D. Yilmaz, K. Yilmaz, Effects of chemical treatments and degumming methods on physical and mechanical properties of okra bast and corn husk fibers, *J. Text. Inst.* (2019) 1–18, <https://doi.org/10.1080/00405000.2019.1702492>.
- [24] D. Klemm, F. Kramer, S. Moritz, T. Lindström, M. Ankerfors, D. Gray, A. Dorris, Nanocelluloses: a new family of nature-based materials, *Angew. Chem. Int. Ed.* (2011) 5438–5466, <https://doi.org/10.1002/anie.201001273>.
- [25] H. Ma, B. Zhou, H.S. Li, Y.Q. Li, S.Y. Ou, Green composite films composed of cellulose nanocrystals and a cellulose matrix regenerated from functionalized ionic liquid solution, *Carbohydr. Polym.* 84 (2011) 383–389, <https://doi.org/10.1016/j.carbpol.2010.11.050>.
- [26] S. Nie, K. Zhang, X. Lin, C. Zhang, D. Yan, H. Liang, S. Wang, Enzymatic pretreatment for the improvement of dispersion and film properties of cellulose nanofibrils, *Carbohydr. Polym.* 181 (2018) 1136–1142, <https://doi.org/10.1016/j.carbpol.2017.11.020>.
- [27] T. Saito, M. Hirota, N. Tamura, S. Kimura, H. Fukuzumi, L. Heux, A. Isogai, Individualization of nano-sized plant cellulose fibrils by direct surface carboxylation using tempo catalyst under neutral conditions, *Biomacromolecules* 10 (2009) 1992–1996, <https://doi.org/10.1021/bm900414t>.
- [28] S.Y. Lee, S.J. Chun, I.A. Kang, J.Y. Park, Preparation of cellulose nanofibrils by high pressure homogenizer and cellulose-based composite films, *J. Ind. Eng. Chem.* 15 (2009) 50–55, <https://doi.org/10.1016/j.jiec.2008.07.008>.
- [29] S. Nie, C. Zhang, Q. Zhang, K. Zhang, Y. Zhang, P. Tao, S. Wang, Enzymatic and cold alkaline pretreatments of sugarcane bagasse pulp to produce cellulose nanofibrils using a mechanical method, *Ind. Crop. Prod.* 124 (2018) 435–441, <https://doi.org/10.1016/j.indcrop.2018.08.033>.
- [30] T. Kos, A. Anzlovar, M. Kunaver, M. Huskic, E. Zagar, Fast preparation of cellulose nanocrystals by microwave-assisted hydrolysis, *Cellulose* 21 (2014) 2579–2585, <https://doi.org/10.1007/s10570-014-0315-2>.
- [31] F. Beltramino, M.B. Roncero, A.L. Torres, T. Vidal, C. Valls, Optimization of sulfuric acid hydrolysis conditions for preparation of cellulose nanocrystals from enzymatically pretreated fibers, *Cellulose* 23 (2016) 1777–1789, <https://doi.org/10.1007/s10570-016-0897-y>.
- [32] B. Li, W. Xu, D. Kronlund, A. Mäeattänen, J. Liu, Jan-Henrik Smått, J. Peltonen, S. Willför, X. Mu, C. Xu, Cellulose nanocrystals prepared via formic acid hydrolysis followed by TEMPO-mediated oxidation, *Carbohydr. Polym.* 133 (2015) 605–612, <https://doi.org/10.1016/j.carbpol.2015.07.033>.
- [33] A.A. Oun, J.W. Rhim, Effect of post-treatments and concentration of cotton linter cellulose nanocrystals on the properties of agar-based nanocomposite films, *Carbohydr. Polym.* 134 (2015) 20–29, <https://doi.org/10.1016/j.carbpol.2015.07.053>.
- [34] Y.J. Tang, X.C. Shen, J.H. Zhang, D.L. Guo, F.G. Kong, N. Zhang, Extraction of cellulose nano-crystals from old corrugated container fiber using phosphoric acid and enzymatic hydrolysis followed by sonication, *Carbohydr. Polym.* 125 (2015) 360–366, <https://doi.org/10.1016/j.carbpol.2015.02.063>.
- [35] F. Shen, W. Xiao, L. Lin, G. Yang, Y. Zhang, S. Deng, Enzymatic saccharification coupling with polyester recovery from cotton-based waste textiles by phosphoric acid pretreatment, *Bioresour. Technol.* 130 (2013) 248–255, <https://doi.org/10.1016/j.biortech.2012.12.025>.
- [36] B.S.L. Brito, F.V. Pereira, J.-L. Putaux, B. Jean, Preparation, morphology and structure of cellulose nanocrystals from bamboo fibers, *Cellulose* 19 (5) (2012) 1527–1536, <https://doi.org/10.1007/s10570-012-9738-9>.
- [37] H. Wang, H. Xie, H. Du, X. Wang, W. Liu, Y. Duan, X. Zhang, L. Sun, X. Zhang, C. Si, Highly efficient preparation of functional and thermostable cellulose nanocrystals via H<sub>2</sub>SO<sub>4</sub> intensified acetic acid hydrolysis, *Carbohydr. Polym.* 239 (2020) 116233, <https://doi.org/10.1016/j.carbpol.2020.116233>.
- [38] H. Xie, Z. Zou, H. Du, X. Zhang, X. Wang, X. Yang, H. Wang, G. Li, L. Li, C. Si, Preparation of thermally stable and surface-functionalized cellulose nanocrystals via mixed H<sub>2</sub>SO<sub>4</sub>/Oxalic acid hydrolysis, *Carbohydr. Polym.* 223 (2019) 115116, <https://doi.org/10.1016/j.carbpol.2019.115116>.
- [39] E. Syafrî, A. Kasim, H. Abrial, A. Asben, Cellulose nanofibers isolation and characterization from ramie using a chemical-ultrasonic treatment, *J. Nat. Fibers* 16 (8) (2019) 1–11, <https://doi.org/10.1080/15440478.2018.1455073>.
- [40] M.M. Rahman, M. Maniruzzaman, M.R. Islam, M.S. Rahman, Synthesis of nano-cellulose from okra fibre and FTIR as well as morphological studies on it, *Am. J. Polym. Sci.* 4 (2018) 42–52, <https://doi.org/10.11648/j.ajpst.20180402.11>.
- [41] K.F. Chung, J. Seiffert, S. Chen, I.G. Theodorou, A.E. Goode, B.F. Leo, C.M. McGilvery, F. Hussain, C. Wiegman, C. Rossios, J. Zhu, J.C. Gong, F. Tariq, V. Yufit, A.J. Monteith, T. Hashimoto, J.N. Skepper, M.P. Ryan, J.F. Zhang, T.D. Tetley, A.E. Porter, Inactivation, clearance, and functional effects of lung-in stilled short and long silver nanowires in rats, *ACS Nano* 11 (3) (2017) 2652–2664, <https://doi.org/10.1021/acsnano.6b07313>.
- [42] M. Roman, Toxicity of cellulose nanocrystals: a review, *Ind. Biotechnol.* 11 (1) (2015) 25–33, <https://doi.org/10.1089/ind.2014.0024>.
- [43] N. Yanamala, E.R. Kisin, A.L. Menas, M.T. Farcas, T.O. Khalilullin, U.B. Vogel, G.V. Shurin, D. Schwegler-Berry, P.M. Fournier, A. Star, A.A. Shvedova, In vitro toxicity evaluation of lignin-(un)coated cellulose based nanomaterials on human A549 and THP-1 cells, *Biomacromolecules* 17 (11) (2016) 3464–3473, <https://doi.org/10.3390/nano12091432>.
- [44] M.T. Hossen, T. Islam, E.I. Mahee, Z.T. Reza, M. Rahman, M.S. Mahmud, A comprehensive study on Physico-Mechanical characteristics of Okra fibre (*Abelmoschus esculentus*) for textile applications, *Indian J. Sci. Technol.* 14 (9) (2021) 765–775, <https://doi.org/10.17485/IJST/v14i9.2268>.
- [45] N. Vasugi, S. Amsamani, R. Sunitha, Extraction and evaluation of OKRA fibres, *Int. J. polymer text. engg (SSRG-IJPTE)*. 6 (1) (2019) 24–30, <https://doi.org/10.14445/23942592/IJPTE-V6I1P105>.
- [46] R. Kusmono, Faiz Listyanda, Muhammad Waziz Wildan, Mochammad Noer Ilman, Preparation and characterization of cellulose nanocrystal extracted from ramie fibers by sulfuric acid hydrolysis, *Heliyon* 6 (11) (2020), <https://doi.org/10.1016/j.heliyon.2020.e05486>.
- [47] R. Faiz Listyanda, Kusmono, Muhammad Waziz Wildan, Mochammad Noer Ilman, Extraction and characterization of nanocrystalline cellulose (NCC) from ramie fiber by sulphuric acid hydrolysis, *AIP Conf. Proc.* 2217 (1) (2020) 030069, <https://doi.org/10.1063/5.0001068>.
- [48] M.M. Khan, T.F. Susmi, M. Miah, M.A. Reza, M.S. Rahi, Morphological alteration and intracellular ROS generation confirm apoptosis induction on EAC cells by leucas indica bark extract, *J. Herbs, Spices, Med. Plants* 29 (1) (2023 Jan 2) 84–97, <https://doi.org/10.1080/10496475.2022.2103765>.
- [49] A. Jabbar, J.Í. Militký, J. Wiener, B.M. Kale, U. Ali, S. Rwawiire, Nanocellulose coated woven jute/green epoxy composites: characterization of mechanical and dynamic mechanical behavior, *Compos. Struct.* (2016) 340–349, <https://doi.org/10.1016/j.compstruct.2016.11.062>.
- [50] J.I. Morán, V.A. Alvarez, V.P. Cyras, et al., Extraction of cellulose and preparation of nanocellulose from sisal fibers, *Cellulose* 15 (2008) 149–159, <https://doi.org/10.1007/s10570-007-9145-9>.
- [51] Z. Li, L. Zhu, H. Zhang, J. Yang, J. Zhao, D. Du, J. Meng, F. Yang, Y. Zhao, J. Sun, Protective effect of a polysaccharide from stem of *Codonopsis pilosula* against renal ischemia/reperfusion injury in rats, *Carbohydr. Polym.* 90 (4) (2012) 1739–1743, <https://doi.org/10.1016/j.carbpol.2012.07.062>.
- [52] R.A. Ilyas, S.M. Sapuan, M.R. Ishak, Isolation and characterization of nanocrystalline cellulose from sugar palm fibres (*Arenga Pinnata*), *Carbohydr. Polym.* 181 (2018) 1038–1051, <https://doi.org/10.1016/j.carbpol.2017.11.045>.
- [53] Y. Habibi, I. Hoeger, S.S. Kelley, O.J. Rojas, Development of Langmuir-Schaeffer cellulose nanocrystal monolayers and their interfacial behaviors, *Langmuir* 26 (2) (2010) 990–1001, <https://doi.org/10.1021/la902444x>.
- [54] M.A. Martins, E.M. Teixeira, A.C. Correa, M. Ferreira, L.H.C. Mattoso, Extraction and characterization of cellulose whiskers from commercial cotton fibers, *J. Mater. Sci.* 46 (2011) 7858–7864, <https://doi.org/10.1007/s10853-011-5767-2>.
- [55] M.I. Voronova, O.V. Surov, S.S. Guseinov, V.P. Barannikov, A.G. Zakharov, Thermal stability of composites of polyvinyl alcohol with nanocrystalline cellulose composites, *Carbohydr. Polym.* 130 (2015) 440–447, <https://doi.org/10.1016/j.carbpol.2015.05.032>.
- [56] Z. Wang, Z. Yao, J. Zhou, M. He, Q. Jiang, S. Li, Y. Ma, M. Liu, S. Luo, Isolation and characterization of cellulose nanocrystals from pueraria root residue, *Int. J. Biol. Macromol.* 129 (2019) 1081–1089, <https://doi.org/10.1016/j.ijbiomac.2018.07.055>.
- [57] J. Lamaming, R. Hashim, O. Sulaiman, C.P. Leh, T. Sugimoto, N.A. Nordin, Cellulose nanocrystals isolated from oil palm trunk, *Carbohydr. Polym.* 127 (2015) 202–208, <https://doi.org/10.1016/j.carbpol.2015.03.043>.
- [58] A. Tiwari, L.H. Hihara, Thermal stability and thermokinetics studies on silicone ceramer coatings: Part 1-inert atmosphere parameters, *Polym. Degrad. Stabil.* 94 (2009) 1754–1771, <https://doi.org/10.1016/j.polymdegradstab.2009.06.010>.
- [59] D. Ye, J. Yang, Ion-responsive liquid crystals of cellulose nanowhiskers grafted with acrylamide, *Carbohydr. Polym.* 134 (2015) 458–466, <https://doi.org/10.1016/j.carbpol.2015.08.025>.

- [60] F. Jiang, Y.L. Hsieh, Chemically and mechanically isolated nanocellulose and their self-assembled structures, *Carbohydr. Polym.* 95 (2013) 32–40, <https://doi.org/10.1016/j.carbpol.2013.02.022>.
- [61] Q. Tarrés, R. Aguado, J.O. Zoppe, P. Mutjé, N. Fiol, M. Delgado-Aguilar, Dynamic light scattering plus scanning Electron microscopy: usefulness and limitations of a simplified estimation of nanocellulose dimensions, *Nanomaterials* 12 (23) (2022) 4288, <https://doi.org/10.3390/nano12234288>.
- [62] Ning Lin, Alain Dufresne, Nanocellulose in biomedicine: current status and future prospect, *Eur. Polym. J.* 59 (2014) 302–325, <https://doi.org/10.1016/j.eurpolymj.2014.07.025>.